



Journal of Applied and Computational Mechanics



Research Paper

Metal and Metallic Oxide Nanofluid over a Shrinking Surface with Thermal Radiation and Heat Generation/Absorption

R.P. Sharma¹, S.R. Mishra²

¹ Department of Mechanical engineering, National Institute of Technology Arunachal Pradesh, Yupia, Papum Pare District, Arunachal Pradesh, India, Email: rpsharma@nitap.ac.in

² Department of Mathematics, Siksha O Anusandhan Deemed to be University, Khandagiri Square, Bhubaneswar, 751030, Odisha, India, Email: satyaranjan_mshr@yahoo.co.in

Received March 02 2020; Revised April 22 2020; Accepted for publication May 02 2020.

Corresponding author: S.R. Mishra (satyaranjan_mshr@yahoo.co.in)

© 2022 Published by Shahid Chamran University of Ahvaz

Abstract. In transport as well as manufacturing industries, the two basic aspects are heating and cooling. The use of metal or metallic oxide nanofluids has an effective cooling technique than that of conventional fluids. Therefore, the work is aimed at describing the three-dimensional MHD flow of metal and metallic oxide nanofluids past a stretching/shrinking sheet embedding with a permeable media. Further, thermal properties are enhanced by incorporating heat generation/absorption and radiative heat energy in the heat equation, enhancing the efficiency of temperature profiles. The convective boundary condition for temperature is used, which affects the temperature profile. Suitable similarity transformation is used to transform the governing equations to ordinary differential equations. The approximate analytical solution is obtained for these transformed differential equations employing the Adomian Decomposition Method (ADM). The influences of characterizing parameters are obtained and displayed via graphs, and the computation results of the heat transfer rate for various values of constraints are shown in a table. It is observed that both the momentum and energy profiles decrease with an enhance in the porosity parameter. Also, the fluid temperature decreases with an increasing thermal radiation parameter, but the opposite effect is encountered for the energy generation/absorption parameter.

Keywords: Nanofluid; MHD; Thermal radiation; Heat generation; Porous medium.

1. Introduction

This modern and novel concept of nanofluid offers enchanting the heat transfer properties correlated to the heat transfer base fluid. Due to its varied industrial applications such as liquid cooling, vehicle cooling, biomedical applications, detergency, etc. many researchers have contributed their study in this direction. As per the technical concern in industries, for transportation, manufacturing, electronics, etc. the vital aspect is cooling. Most of the electronics product those are operating a long time they need cooling and for the state of cooling, scientists using nanofluid instead of conventional fluid. As per the biomedical concern, nanofluid is used for drug delivery. Gold nanoparticles are widely useful in sensor field surface modification material of DNA sensors to increase their sensitivity like sensitive membrane preparation. Nanoparticle liquid suspension (Nanofluid) is the term invented by Choi [1] to mark out this novel theory of nanotechnology-based energy transfer fluid that shows thermal properties higher to those of their base liquid. Nanoparticles used in nanofluids have been made of different materials, such as metals (Au, Ag, Cu), carbide ceramics (SiC, TiC), nitride ceramics (SiN, AlN), oxide ceramics (CuO, Al₂O₃), and carbon nanotubes. Nanofluids aim to get the highest feasible thermal properties at the least feasible concentrations (in preference less than 1% by volume) by constant scattering and firm suspension of nanoparticles in base liquids. To attain this aim it is essential to know how nanoparticles improve heat transport in fluids. In the past few years, some attention has been specified convective transport of nanofluids. A wide review of the thermal conductivity of nanofluids has introduced by some researchers (Mishra et al. [2-3]; Parida and Mishra [4]; Bhatti et al. [5] and Makinde and Mishra [6]). Takhar et al. [7] scrutinized the magnetohydrodynamic effect of an unsteady flow due to the impulsive motion in a stretching surface. Free convection of a nanofluid in a nonisothermal vertical plate embedding with a porous medium is investigated by Gorla and Chamkha [8]. Further, Damseh et al. [9] and Zaraki et al. [10] have presented the influences of heat generation/absorption as well as the chemical reaction on the flow of micropolar and nanofluids respectively. Sandeep et al. [11-12]; Das et al. [13-15] have presented their study for the behavior of several physical parameters on the flow of nanofluid in various geometries. They have employed both analytical as well as numerical techniques for the solution of complex governing equations. In a useful discussion, Chamkha [16,17] presented the solar radiation in a free convective flow through a porous medium. For the heat transfer enhancement through a nanofluid, the nanoparticle diameter plays an important role. Ghalambaz et al. [18] carried out their study for the behavior of Al₂O₃-nanoparticle diameter in conjunction with variable thermal conductivity. However, mixed convection of nanofluid for the effect of thermal radiation was conducted by Chamkha et al. [19] and Gorla et al. [20]. In both of the aforementioned studies, authors have considered the flow through the permeable medium. An analysis of water-based nanofluids on the different physical conditions have presented by Sheikholeslami et al. [21, 22] and Salem



et al. [23]. The motion and energy transport of a nanoliquid, considering metallic nanoparticles for the variation of different pertinent parameters was conducted by Chamkha and his co-authors [24-26].

The study of fluid motion with a magnetic field is considered important in the polymer industry, metallurgy, engineering, physics, and chemistry, etc. Also, the MHD flow plays a vital role in problems related to blood plasma, blood pump machines, and physiological fluids. An electrically conducting liquid conditional on a magnetic field is suitable in governing the rate of cooling. The electro-conducting fluid has been increasingly used in the manufacturing processes of semiconducting material such as silicon crystal gallium arsenide. The effect of the magnetic field could be very helpful in the modernization of technological processes. On account of their varied importance, these flows have been studied by several authors, notable amongst them are (Turkyilmazoglu [27]; Hamad [28]; Sheikholeslami et al. [29]; Ibrahim and Makinde [30]).

Radiation is the temperature that originates from a source and travels via some material or space. Sound, energy, and light are the kinds of radiation. The thermal radiation impact might performance an important character in controlling the energy transfer process in the polymer processing industry. Various manufacturing procedures, for example, solar power skill, astrophysical flows, fossil fuel combustion heat processes, gas turbines, the many impulsion devices for missiles, aircraft, satellites, missiles. Also, heat radiation shows a vigorous part in procedures in manufacturing areas that arise at high energy for the design of numerous advanced heat adaptation systems. Several authors analyzed the radiation impact on energy transfer of a nanofluid in different physical conditions, notable amongst them are (Magyari and Chamkha [31]; Nadeem et al. [32,33]; Turkyilmazoglu et al. [34]; Chamkha and Khaled [35]; Ramzan and Bilal [36]; Hayat et al. [37]; Hag et al. [38]). The impacts of energy generation on the assorted convective motion of a nano liquid over a non-linear extending surface were analyzed by Lakshmi et al. [39]. Hayat et al. [40] have analyzed the three-dimensional motion of a nanofluid past an extending sheet.

The motion of liquids past a porous medium is of great importance in heat removal from nuclear fuel debris, underground disposal of radiative waste material storage of foodstuff, and oil exploration. On the porous shrinking sheet, suction/injection of a liquid can noticeably variation the motion arena. Injection of the liquid via a permeable shrinking surface is of mutual apprehension in numerous applications that contain laminar boundary film control applications. These contain the coating of wires, film cooling, polymer fiber coating. Normally, suction is probable to practice the friction factor. Instead, injection acts oppositely. Suction is useful for chemical procedures to eliminate reactants. The injection is utilized to improve reactants, prevent corrosion, reduce the drag and cool the surface and also suction or injection is significant in manufacturing activities for example in the structure of bearings, diffusers, and thermal oil repossession. Malvandi et al. [41] reported the energy generation impact on the stagnation-point motion of a nanofluid past a stretching sheet through porous media. Some authors have studied the motion of a nanoliquid through porous media in different physical conditions, notable amongst them are (Kahar et al. [42]; Rashidi et al. [43]; Sheikholeslami and Ganji [44]). The influence of the magnetic field, Hall current, and heat generation/absorption in free convective flow over a moving vertical plate were conducted by Takhar et al. [45] and Chamkha [46] respectively. Recently, Sharma et al. [47] and Hayat et al. [48] have reported the 3-dimensional flow of a nano liquid past an extending surface for the effects of the heat source.

To the best of our knowledge, the influence of the three-dimensional MHD flow of metal and metallic oxide nanofluids past a stretching/shrinking sheet embedding with a permeable media and convective boundary condition has not been studied before. Therefore, the key goal i.e. the novelty of the present analysis is to form a mathematical model to recognize the influence of radiation on the 3-D MHD motion of metal and metallic oxide nanofluids past a stretching/shrinking sheet embedding with a permeable media with convective boundary condition. Due to the higher thermal conductivity of both the metal and metallic oxide nanoparticles, the cooling efficiency also enhances. However, one more novelty is the solution procedure. Instead of traditional numerical methods, we have employed a semi-analytical technique i.e. Adomian Decomposition Method (ADM). The structures of the motion and energy transfer features are studied through designing diagrams, tables, and analyzed in detail. This work is established as follows: In Section 2, the problem formalism. Section 3 includes the solution of the problem by the Adomian Decomposition Method (ADM). Section 4 contains a discussion and results. The conclusions are reviewed in Section 5.

2. Mathematical Modeling and Formulation

Radiative three-dimensional motion of a viscous nanoliquid in a conducting medium over a shrinking sheet is considered in the present investigation. The motion over a permeable media is considered with an added heat source in the energy equation. The conducting fluid-induced with the magnetic field act normal to xy -plane with field strength B_0 (Fig.1). However, assuming the small magnetic Reynolds number, the induced electric current, as well as Hall current effects, are neglected.

Following aforesaid assumptions, the flow phenomena associated with the problem can be described as:

$$\frac{\partial u}{\partial x} + \frac{\partial v}{\partial y} + \frac{\partial w}{\partial z} = 0 \quad (1)$$

$$\rho_{nf} \left(u \frac{\partial u}{\partial x} + v \frac{\partial u}{\partial y} + w \frac{\partial u}{\partial z} \right) = \mu_{nf} \frac{\partial^2 u}{\partial z^2} - \sigma B_0^2 u - \frac{\mu_{nf}}{K_p} u \quad (2)$$

$$\rho_{nf} \left(u \frac{\partial v}{\partial x} + v \frac{\partial v}{\partial y} + w \frac{\partial v}{\partial z} \right) = \mu_{nf} \frac{\partial^2 v}{\partial z^2} - \sigma B_0^2 v - \frac{\mu_{nf}}{K_p} v \quad (3)$$

$$u \frac{\partial T}{\partial x} + v \frac{\partial T}{\partial y} + w \frac{\partial T}{\partial z} = \alpha_{nf} \left(1 + \frac{16 \sigma^* T_\infty^3}{3k_{nf} k} \right) \frac{\partial^2 T}{\partial z^2} + \frac{Q_0}{(\rho C_p)_{nf}} (T - T_\infty) \quad (4)$$

The relevant conditions are

$$u = cx, v = c(m_2 - 1)y, w = -W, -k_f \frac{\partial T}{\partial z} = h_1 (T_f - T) \quad \text{at } z = 0 \quad (5)$$

$$u = 0, v = 0, T \rightarrow T_\infty \quad \text{at } z \rightarrow \infty$$



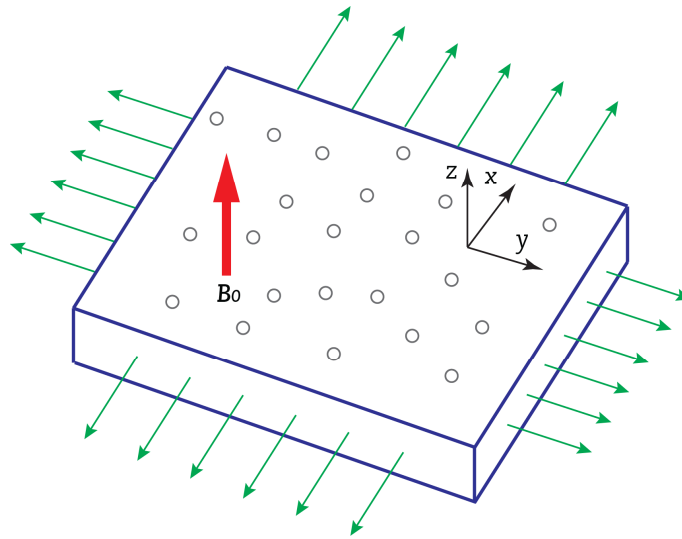


Fig. 1. Flow diagram

where $\alpha_{nf} = k_{nf} / (\rho Cp)_{nf}$ is the thermal diffusivity, $\rho_{nf} = \rho_f(1 - \phi) + \rho_s\phi$, the density, using Gherasim et al. [50] $\mu_{nf} = 0.904e^{14.8\phi} \mu_f$, the viscosity, $(\rho Cp)_{nf} = (\rho Cp)_f(1 - \phi) + (\rho Cp)_s\phi$, the heat capacitance, following Mintsa et al.[51] $k_{nf} = k_f(1.72\phi + 1.0)$, the thermal conductivity is chosen for the effective physical properties of nanofluid. Here, the convective thermal condition is presented with the coefficient h_1 , the suction velocity, W , the rate constant, $c < 0$. In particular $m_2 = 0$, the sheet shrinks along the flow direction (x-direction) also for $m_2 = 2$ the sheet shrinks axis-symmetrically (Zheng et al. [49]).

We now present [49] the subsequent dimensionless parameters and similarity transformations:

$$\theta(\eta) = \frac{T - T_\infty}{T_f - T_\infty}, w = -\sqrt{bv_f} m_2 f(\eta), u = bx f'(\eta), v = b(m_2 - 1)y f'(\eta), \eta = \sqrt{\frac{b}{v_f}} z \tag{6}$$

where prime denotes the differentiation w.r.to η , using Eq. (6), the Eq. (1) is identically satisfied, and substituting into Eqs. (2, 3 and 4) we obtain

$$\frac{0.904e^{14.8\phi}}{1 - \phi + \frac{\rho_s}{\rho_f}\phi} f''' + m_2 f f'' - f'^2 - M \frac{1}{1 - \phi + \frac{\rho_s}{\rho_f}\phi} f' - Pr \chi \frac{0.904e^{14.8\phi}}{1 - \phi + \frac{\rho_s}{\rho_f}\phi} f' = 0 \tag{7}$$

$$\frac{1}{1 - \phi + \frac{(\rho cp)_s}{(\rho cp)_f}\phi} \left((1.72\phi + 1.0) + \frac{4}{3} Nr \right) \theta'' + Pr m_2 f \theta' + Pr \frac{1}{\left(1 - \phi + \frac{(\rho cp)_s}{(\rho cp)_f}\phi \right)} Q \theta = 0 \tag{8}$$

The boundary conditions (5), reduce to

$$\left. \begin{aligned} f(0) = S, f'(0) = \delta, \theta'(0) = -Bi[1 - \theta(0)] \\ f'(\infty) \rightarrow 0, \theta(\infty) \rightarrow 0 \end{aligned} \right\} \tag{9}$$

where $Nr = 4\sigma^* T_\infty^3 / k_{nf} k^*$, the radiation parameter, $M = \sigma B_0^2 / \rho_f b$ (magnetic parameter), $Q = Q_0 / b(\rho Cp)_f$, the heat source parameter, $Pr = v_f(\rho Cp)_f / k_f$, the Prandtl number, $\delta = c / b$ (stretching/shrinking parameter), $S = W / \sqrt{bv_f} m_2$ (suction/injection parameter), $\chi = \alpha_f / bKp^*$ (porosity parameter), $Bi = h_1 \sqrt{v/b} / k$, the Biot number.

3. Solution of the Problem

The system of DEs (7), (8) with the boundary conditions (9) are solved by employing the Adomian Decomposition Method (ADM). Using the general formulation of ADM we have to introduce the operators $\ell_1 = d^3/d\eta^3$ and $\ell_2 = d^2/d\eta^2$ with inverse operators $\ell_1^{-1}() = \int_0^\eta \int_0^\eta \int_0^\eta () d\eta d\eta d\eta$ and $\ell_2^{-1}() = \int_0^\eta \int_0^\eta () d\eta d\eta$. Thus, Eqns. (7)-(8) can be expressed as follows:

$$f(\eta) = -\frac{1 - \phi + \frac{\rho_s}{\rho_f}\phi}{0.904e^{14.8\phi}} \ell_1^{-1} \left(m_2 f f'' - f'^2 - M \frac{1}{1 - \phi + \frac{\rho_s}{\rho_f}\phi} f' - Pr \chi \frac{0.904e^{14.8\phi}}{1 - \phi + \frac{\rho_s}{\rho_f}\phi} f' \right) \tag{10}$$



$$\theta(\eta) = - \frac{\left(1 - \phi + \frac{(\rho c p)_s}{(\rho c p)_f} \phi\right)}{\left(\frac{3N_R + 4}{3N_R}\right) + (1.72\phi + 1.0)} \ell_2^{-1} \left[\Pr m_2 f \theta' + \Pr \frac{1}{\left(1 - \phi + \frac{(\rho c p)_s}{(\rho c p)_f} \phi\right)} Q \theta \right] \tag{11}$$

The linear and nonlinear terms of the above equations can be treated as an infinite series of polynomials of the form:

$$\sum_{m=0}^{\infty} A_m = f f'', \sum_{m=0}^{\infty} B_m = f'^2, \sum_{m=0}^{\infty} C_m = f', \sum_{m=0}^{\infty} D_m = f \theta', \sum_{m=0}^{\infty} E_m = \theta \tag{12}$$

The exact solutions of (7) -(8) are as follows:

$$f(\eta) = \text{Lim} \sum_{m=0}^{\infty} f_m, \text{ and } \theta(\eta) = \text{Lim} \sum_{m=0}^{\infty} \theta_m \tag{13}$$

The initial guess solutions and the successive order solutions are given as follows:

$$f_0(\eta) = S + \delta \eta + \frac{1}{2} p \eta^2 \tag{14}$$

$$\theta_0(\eta) = 1 + \left(1 + \frac{1}{Bi}\right) \eta \tag{15}$$

and

$$f_{m+1}(\eta) = - \frac{1 - \phi + \frac{\rho_s}{\rho_f} \phi}{0.904e^{14.8\phi}} \ell_1^{-1} \left[m_2 A_m - B_m - M \frac{1}{1 - \phi + \frac{\rho_s}{\rho_f} \phi} C_m - \Pr \chi \frac{0.904e^{14.8\phi}}{1 - \phi + \frac{\rho_s}{\rho_f} \phi} C_m \right] \tag{16}$$

$$\theta_{m+1}(\eta) = - \frac{\left(1 - \phi + \frac{(\rho c p)_s}{(\rho c p)_f} \phi\right)}{\left(\frac{3N_R + 4}{3N_R}\right) + (1.72\phi + 1.0)} \ell_2^{-1} \left[\Pr m_2 D_m + \Pr \frac{1}{\left(1 - \phi + \frac{(\rho c p)_s}{(\rho c p)_f} \phi\right)} Q E_m \right] \tag{17}$$

Using $m=0,1,2,\dots$ and evaluating the unknowns p and q we get the particular solutions. The local Nusselt number is described as follows:

$$Nu = \frac{x q_w}{k_f (T_f - T_\infty)} \tag{18}$$

From equations (6) and (8) we obtain.

$$Nu Re^{-1/2} = - \left(\frac{k_{nf}}{k_f} + \frac{4}{3} Nr \right) \theta'(0) \tag{19}$$

where q_w is the surface heat flux and $Re_x = u_w x / \nu_f$ (Local Reynolds number).

Table 1. Thermophysical properties of water and nanoparticles

	ρ (Kg/m ³)	C_p (J/Kgk)	k (W/m.k)
Pure Water	997.1	4179	0.613
Copper (Cu)	8933	385	401
Alumina (Al ₂ O ₃)	3970	765	40

4. Results and Discussion

To study the nature of the velocity and temperature distribution for Cu-H₂O as well as Al₂O₃-H₂O based nanofluids, mathematical calculations are completed for the different values of $M, \chi, Nr, S, Q, \delta, Bi$ and ϕ which are enumerated in figures. Inclusive solutions were attained and are introduced in Figs. 2–13. At the period of calculation, the fixed values of different variables $M = 1; m_2 = 1; \chi = 0; Pr = 6.2; Nr = 0; S = 0.1; Q = -0.1; \delta = 1; Bi = 0.5$ are assumed excluding for the variation of the variables matching to the corresponding figures. Now attained the mathematical result for various parameters, namely nanoparticle volume fraction (ϕ), Biot number (Bi), shrinking parameter (δ), radiation parameter (Nr), heat source/sink parameter (Q), magnetic parameter (M), suction parameter (S), and porosity parameter (χ), etc.

4.1 Velocity distribution

Fig. 2 depicts the impact of nanoparticle volume fraction on the momentum. The present figure describes the influence of both the absence of volume fraction (pure fluid, blue lines) i.e. $\phi = 0$ and various values of volume fraction of Cu and Al₂O₃ nanoparticles. The volume fraction is the amount of nanoparticles i.e. the percentage of nanoparticle accounted for in a certain volume of the



base fluid. It is noted that, in the case of pure fluid, the profile is closed towards the sheet and further it enhances the thickness of the boundary layer in the entire region. In close comparison between the two nanoparticles, it is clear that Cu-water nanofluid (black lines) reduces the profile more than the profiles of Al₂O₃-water nanofluids (red lines). The fact is, due to the higher density of Cu than the Al₂O₃ nanoparticles more amount of particle is clogged near the sheet for which velocity reduces. Fig. 3 illustrates the influences of the magnetic parameter on the velocity profiles using Cu and Al₂O₃-water nanofluids along with the case of pure fluid. The profile exhibited for the absence of porosity parameter. It is noted that, as the magnitude of such parameters increases, the velocity diminishes. The reason is that the growing value of magnetic parameter parameters induces the Lorentz force, a resistive force that resists the fluid motion. Again, it is seen that Cu-water nanoparticles have a more retarding effect than that of Al₂O₃-water nanofluid in conjunction with magnetic parameter. The one more resistive force i.e. the influence of porosity is displayed on the velocity distribution in the presence of the magnetic parameter in Fig. 4. The figure shows in the absence of porosity maximum velocity is exhibited in the boundary layer and for enhances in a porous matrix, the velocity retards. The inclusion of both the resistive forces has retarding effects to reduce the thickness of the profile. With the inclusion of magnetic and porosity parameters Fig. 5 portrays the behavior of suction on the velocity in both the occurrence of nanofluids. It is seen that fluid will exert from the higher-pressure region to lower pressure region for which the thickness of the profiles reduces, as a result, the velocity decreases. The Cu-water nanofluid dominants over Al₂O₃ so that the retardation is maximum. It is interesting to observe that, in the case of impermeable ($S = 0$), maximum velocity exhibited in the entire flow domain. Fig. 6 describes the effect of δ , the velocity ratio on the momentum. The sign '+/-' represents the stretching/shrinking cases respectively. The dual character in the profile is exhibited for both cases. However, it is noted that, as the δ rises in magnitude, the momentum increases.

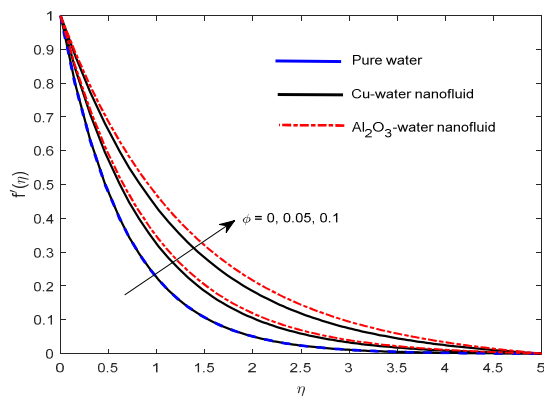


Fig. 2. Velocity descriptions for different values of nanoparticle volume fraction
 $M = 1; m_2 = 1; \chi = 0; Pr = 6.2; Nr = 0; S = 0.1; Q = -0.1; \delta = 1; Bi = 0.5$

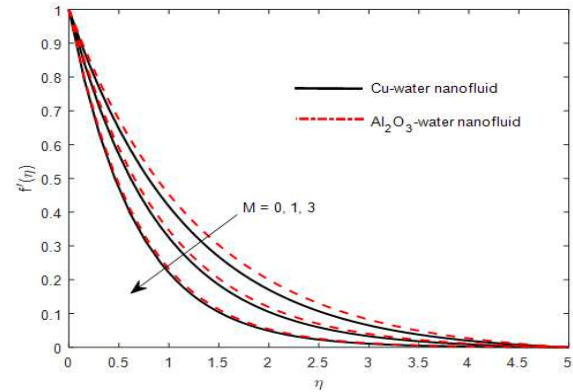


Fig. 3. Velocity descriptions for dissimilar values of the magnetic parameter
 $m_2 = 1; \chi = 0; Pr = 6.2; Nr = 0; S = 0.1; Q = -0.1; \delta = 1; Bi = 0.5; \phi = 0.05$

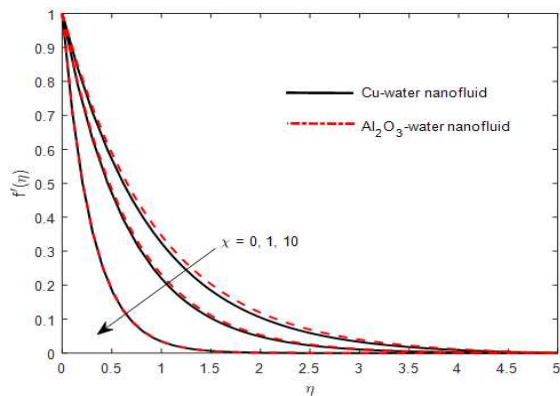


Fig. 4. Velocity profiles for various values of porosity parameter
 $M = 1; m_2 = 1; Pr = 6.2; Nr = 0; S = 0.1; Q = -0.1; \delta = 1; Bi = 0.5$

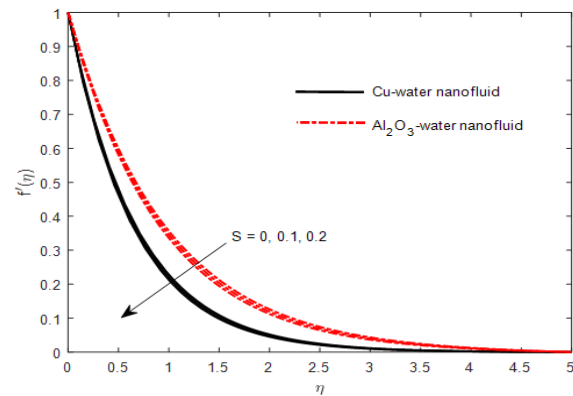


Fig. 5. Velocity profiles for various values of the suction parameter
 $M = 1; m_2 = 1; \chi = 1; Pr = 6.2; Nr = 0; Q = -0.1; \delta = 1; Bi = 0.5; \phi = 0.05$

4.2 Temperature distribution

Figure 7 displays the impact of ϕ , the nanoparticle volume fraction on the energy distributions. It is noticed that as the ϕ enhances, the energy upsurges because when the ϕ rises, the thermal conductivity upsurges, and the thickness of the thermal boundary layer depresses. It is also observed that the variation from the negative region towards the positive region enhances with the decrease in magnitude for which the thickness retards. From the figure, it is seen that, the pure fluid case maximum temperature exhibited, and in comparison, to both of the nanoparticles, Cu-water nanofluid has a dominating role over the Al₂O₃ nanofluid. The fact is, the conductivity of Cu is more for which the capacity for heat transfer enhances. Figs. 8 and 9 illustrate the impact of the magnetic parameter and porosity parameter on the energy description respectively. It is noted that for the growing value of the magnetic parameter and porosity parameter the energy description diminishes. The reason is the stored energy dissipates from the plate region towards the fluid region for which a similar trend in the profile is marked. Fig. 10 explains the effect of the suction parameter on the energy description. It is observed that for the growing value of suction parameter energy profile upsurges. It is seen that in the impermeable case i.e. when ($S = 0$) the fluid exhibits its maximum temperature. However, in the case of Cu-eater nanofluid, the rate of enhancing is more significant than that of the case of Al₂O₃-water nanofluid. The effects of the heat source/sink parameter on the temperature profile are seen in Fig. 11. Moreover, the absence case i.e. $Q = 0$ is also presented in the same figure.



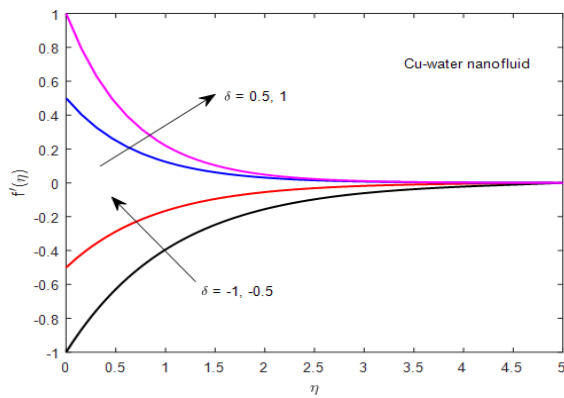


Fig. 6. Velocity descriptions for dissimilar values of the shrinking parameter

$M = 1; m_2 = 1; \chi = 1; Pr = 6.2; Nr = 0; Q = -0.1; S = 0.1; Bi = 0.5; \phi = 0.05$

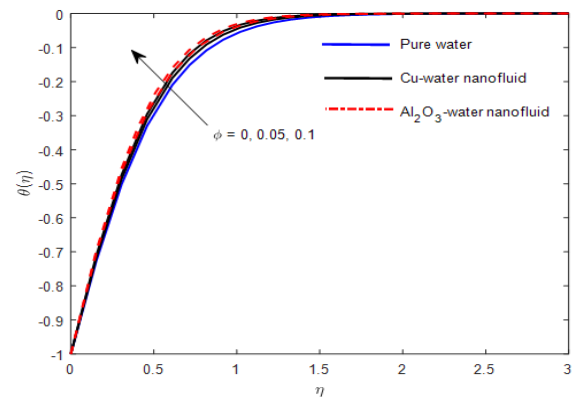


Fig. 7. Temperature profiles for various values of nanoparticle volume fraction

$M = 1; m_2 = 1; \chi = 0; Pr = 6.2; Nr = 0; Q = -0.1; S = 0.1; \delta = 1; Bi = 0.5$

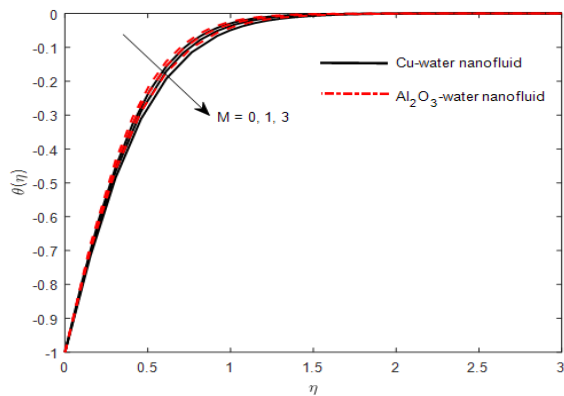


Fig. 8. Temperature descriptions for dissimilar values of magnetic parameter

$m_2 = 1; \chi = 0; Pr = 6.2; Nr = 0; Q = -0.1; S = 0.1; \delta = 1; Bi = 0.5; \phi = 0.05$

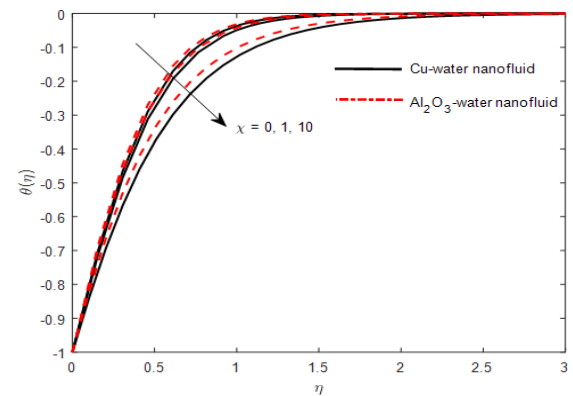


Fig. 9. Temperature descriptions for various values of porosity parameter

$M = 1; m_2 = 1; Pr = 6.2; Nr = 0; Q = -0.1; S = 0.1; \delta = 1; Bi = 0.5; \phi = 0.05$

Noticeable increase in fluid temperature is marked from the sink to source in the entire thermal layer and comparison to both the nanofluids, it is observed that the nature of Cu nanoparticle always dominates over the Al_2O_3 nanoparticles. The behavior of Biot number (Bi) i.e. due to the heat flux on the fluid temperature is displayed in Fig. 12. Due to the uniform temperature field inside the body, the values considered for the Biot number makes the problem thermally simple. For $Bi < 0.1$ the heat conduction is much faster than heat convection away from its surface. It is because of the lesser temperature gradients inside the body. Here, it is seen that within this range increasing Bi enhances the profile as well. The performance of the Nr on the energy description is seen in Fig. 13. It is detected that the thermal radiation yields a diminution in the energy profile because the thermal radiation parameter diminishes the thickness of the thermal boundary layer.

4.3 Numerical simulation of engineering coefficients

Table 2 displays the numerical computation for the behavior of several parameters on the rate of heat transfer coefficient described through Nusselt number i.e. $Nu(Re_x)^{-1/2}$. We observed that the value of $Nu(Re_x)^{-1/2}$ upsurges in magnitude for growing the values of nanoparticle volume fraction as well as the thermal radiation. However, for the magnetic, porosity, heat sink to source, and the enhanced values of Biot number the effect is reversed. Moreover, it is to note that due to a good conductor of heat transfer Cu nanoparticle also dominates over the Al_2O_3 from each case. Therefore, it is the suggestive measure to care for the choice of nanoparticles for the enhanced heat transfer rate for various industrial purposes.

Table 2. Value of Nusselt number for $Pr = 6.2; S = 0.1; \delta = 1$

ϕ	M	χ	Q	Nr	Bi	Cu -water	Al_2O_3 -water
0	1	0	0	0	0.5	-2.1613	-2.1613
0.05						-2.2265	-2.2332
0.1						-2.2755	-2.2787
0.05	2					-2.1825	-2.187
	3					-2.1449	-2.148
	1	1				-2.1442	-2.1473
		10				-1.7868	-1.784
		1	-0.3			-2.6198	-2.6208
			-0.1			-2.3142	-2.3164
			0.1			-1.9588	-1.9631
			0.3			-1.5209	-1.53
			0.1	1		-2.3943	-2.4123
				2		-2.5926	-2.6227
				1	0.3	-1.0261	-1.0339
					0.1	-0.266	-0.268



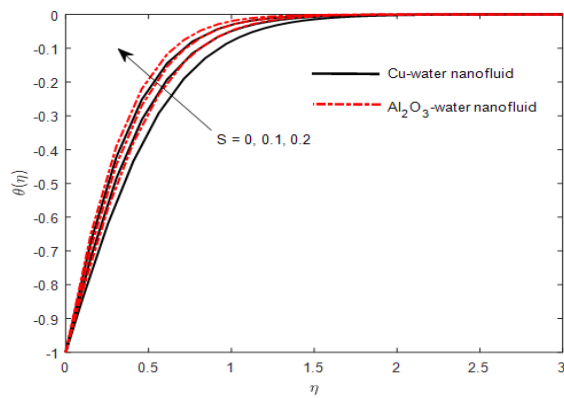


Fig. 10. Temperature descriptions for various values of the suction parameter

$M = 1; \chi = 1; m_2 = 1; Pr = 6.2; Nr = 0; Q = -0.1; \delta = 1; Bi = 0.5; \phi = 0.05$

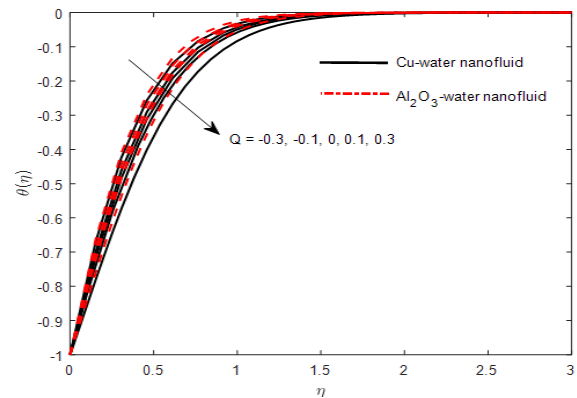


Fig. 11. Temperature description for dissimilar values of Q ,

$M = 1; \chi = 1; m_2 = 1; Pr = 6.2; Nr = 0; S = 0.1; \delta = 1; Bi = 0.5; \phi = 0.05$

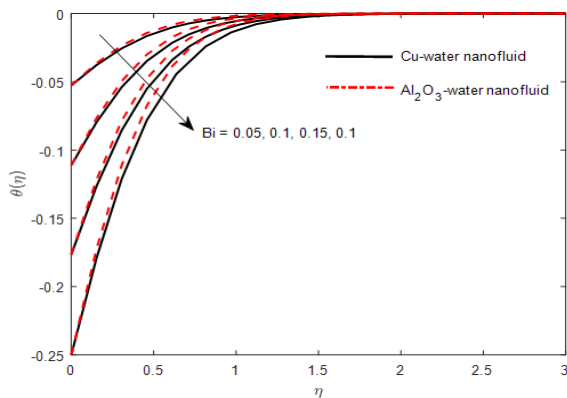


Fig. 12. Temperature profiles for various values of Biot number

$M = 1; \chi = 1; m_2 = 1; Pr = 6.2; Nr = 0; S = 0.1; \delta = 1; Q = 0.1; \phi = 0.05$

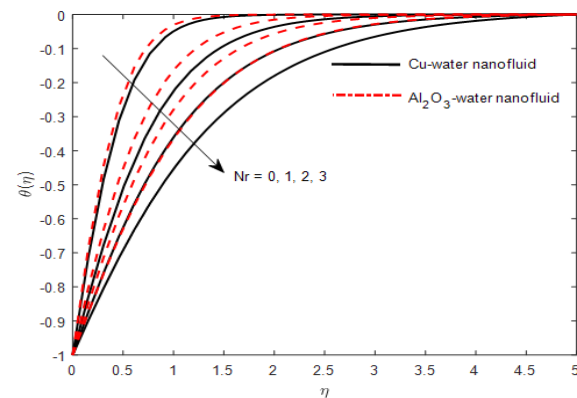


Fig. 13. Temperature descriptions for unlike values of radiation parameter

$M = 1; \chi = 1; m_2 = 1; Pr = 6.2; Q = 0.1; S = 0.1; \delta = 1; Bi = 0.5; \phi = 0.05$

5. Conclusion

In the present study, the magnetohydrodynamic 3-dimensional flow of nano liquid over a shrinking surface under the effect of thermal radiation and heat generation via the permeable media was investigated. The physical effects of distinct parameters such as nanoparticle volume fraction, Biot number, radiation parameter, magnetic parameter, porosity parameter, shrinking parameter, heat source/sink parameter and, suction parameter on momentum and energy descriptions were depicted and discoursed in this paper. The main observations are listed below.

- The effects of magnetic parameter M , suction parameter S , and permeability parameter χ on the velocity description f' are similar.
- The velocity description f' enhances when ϕ and shrinking parameter δ enhances.
- The effects of magnetic parameter M , Radiation parameter Nr , porosity parameter χ , heat source/sink parameter Q , and Biot number Bi on the temperature profile θ are similar.
- The temperature profile θ decreases when the Nr increases.
- The temperature description θ rises when the ϕ and the suction parameter enhances.

Author Contributions

R.P. Sharma planned the scheme, initiated the work and suggested the model; S.R. Mishra conducted the methodology and examined the theoretical validation of the manuscript and all authors discussed the results, reviewed and approved the final version of the manuscript.

Acknowledgments

We are very much thankful to the learned reviewers for their qualitative suggestions to improve the quality of our manuscript.

Conflict of Interest

The authors declared no potential conflicts of interest with respect to the research, authorship and publication of this article.

Funding

The authors received no financial support for the research, authorship and publication of this article.



Data Availability Statements

The datasets generated and/or analyzed during the current study are available from the corresponding author on reasonable request.

Nomenclature

B_0	Magnetic field strength	Kp^*	Porosity in dimensional form
T	Fluid temperature	u, v, w	Velocity components along x, y and z directions
T_∞	Free stream temperature	Greek symbols	
c	Rate constant	f	Non-dimensional stream function
k^*	Mean absorption coefficient	θ	Non-dimensional temperature
Q	Heat source/sink	ϕ	Nanoparticle volume fraction
k	Thermal conductivity	α	Thermal diffusivity
C_p	Specific heat	ρ	Fluid density
U_w	Stretching velocity	σ^*	Stephan-Boltzmann constant
U_0	Reference velocity	ν	Kinematic viscosity
L	Characteristic length	μ	Dynamic viscosity
M	Magnetic field parameter	χ	Non-dimensional porosity
Pr	Prandtl number	Subscripts	
R	Thermal radiation	f	Base fluid
W	Suction velocity	nf	Nanofluid


References


- [1] Choi, S.U.S., Enhancing thermal conductivity of fluids with nanoparticles, in *proc. ASME Int. mechanical engineering Congress and exposition ASME, FED 231/MD 66*, 1995, 99-105.
- [2] Mishra, S.R., Nayak, B., Sharma, R.P., MHD stagnation-point flow over a stretching sheet in the presence of non-Darcy porous medium and heat source/sink, *Defect and Diffusion Forum*, 374, 2017, 92-105.
- [3] Mishra, S.R., Rout, B.C., Analytical solution of electrical conducting water-based (KKL model) nanofluid flow over a linearly stretching sheet, *Iranian Journal of Science and Technology, Transactions A: Science*, 43, 2019, 1239-1247.
- [4] Parida, S.K., Mishra, S.R., Heat and mass transfer of MHD stretched nanofluids in the presence of chemical reaction, *Journal of Nanofluids*, 8(1), 2019, 143-149.
- [5] Bhatti, M. M., Mishra, S. R., Abbas, T., Rashidi, M. M., A mathematical model of MHD nanofluid flow having gyrotactic microorganisms with thermal radiation and chemical reaction effects, *Neural Computing and Applications*, 30, 2018, 1237-1249.
- [6] Makinde, O. D., Mishra, S. R., On stagnation point flow of variable viscosity nanofluids past a stretching surface with radiative heat, *International Journal of Applied and Computational Mathematics*, 3(2), 2017, 561-578.
- [7] Takhar, H. S., Chamkha, A. J., Nath, G., Unsteady three-dimensional MHD-boundary-layer flow due to the impulsive motion of a stretching surface, *Acta Mechanica*, 146, 2001, 59-71.
- [8] Gorla, R.S.R., Chamkha, A.J., Natural convective boundary layer flow over a nonisothermal vertical plate embedded in a porous medium saturated with a nanofluid, *Nanoscale and Microscale Thermophysical Engineering*, 15(2), 2009, 81-94.
- [9] Damseh, R. A., Al-Odat, M.Q., Chamkha, A.J., Shannak, B.A., Combined effect of heat generation or absorption and first-order chemical reaction on micropolar fluid flows over a uniformly stretched permeable surface, *International Journal of Thermal Sciences*, 48(8), 2009, 1658-1663.
- [10] Zaraki, A., Ghalambaz, M., Chamkha, A.J., Ghalambaz, M., Rossi, D.D., Theoretical analysis of natural convection boundary layer heat and mass transfer of nanofluids: effects of size, shape, and type of nanoparticles, type of base fluid and working temperature, *Advanced Powder Technology*, 26(3), 2015, 935-946.
- [11] Sandeep, N., Malvandi, A., Enhanced heat transfer in liquid thin film flow of non-Newtonian nanofluids embedded with graphene nanoparticles, *Advanced Powder Technology*, 27(6), 2016, 2448-2456.
- [12] Sandeep, N., Sharma, R.P., Ferdows, M., Enhanced heat transfer in unsteady magnetohydrodynamic nanofluid flow embedded with aluminum alloy nanoparticles, *Journal of Molecular Liquids*, 234, 2017, 437-443.
- [13] Das, S., Sharma, A.S., Jana, R.N., Sharma, R.P., Slip flow of nanofluid past a vertical plate with ramped wall temperature considering thermal radiation, *Journal of Nanofluids*, 6(6), 2017, 1054-1064.
- [14] Das, S., Sen, A., Jana, R. N., Sharma, R. P., Stability of Nanofluid Flow Through a Vertical Channel with Wall Thermal Conductance and Radiation, *Journal of Nanofluids*, 6(4), 2017, 680-690.
- [15] Das, S., Jana, R. N., Sharma, R. P., Makinde, O. D., MHD nanofluid flow and heat transfer in the Ekman layer on an oscillating porous plate, *Journal of Nanofluids*, 5(6), 2016, 968-981.
- [16] Chamkha, A.J., Solar radiation assisted natural convection in uniform porous medium supported by a vertical flat plate, *Journal of Heat Transfer*, 119(1), 1997, 89-96.
- [17] Chamkha, A.J., Hydromagnetic Natural Convection from an Isothermal Inclined Surface Adjacent to a Thermally Stratified Porous Medium, *International Journal of Engineering Science*, 35(10-11), 1997, 975-986.
- [18] Ghalambaz, M., Behseresh, A., Behseresh, J., Chamkha, A.J., Effects of nanoparticles diameter and concentration on natural convection of the Al₂O₃-water nanofluids considering variable thermal conductivity around a vertical cone in porous media, *Advanced Powder Technology*, 26(1), 2015, 224-235.
- [19] Chamkh, A.J., Abbasbandy, S., Rashad, A. M., Vajravelu, K., Radiation Effects on Mixed Convection over a Wedge Embedded in a Porous Medium Filled with a Nanofluid, *Transport in Porous Media*, 91(1), 2013, 261-279.
- [20] Gorla, R.S.R., Chamkha, A.J., Rashad, A.M., Mixed convective boundary layer flow over a vertical wedge embedded in a porous medium saturated with a nanofluid: Natural convection dominated regime, *Nanoscale Research Letters*, 6, 2011, 207.
- [21] Sheikholeslami, M., Ellahi, R., Ashorynejad, H.R., Donairry, G., Hayat, T., Effects of heat transfer in the flow of nanofluids over a permeable stretching wall in a porous medium, *Journal of Computational and Theoretical Nanoscience*, 11, 2014, 486-496.
- [22] Sheikholeslami, M., Bandpy, M.G., Ganji, D.D., Soleimani, S., Natural convection heat transfer in a cavity with a sinusoidal wall filled with CuO-water nanofluid in presence of the magnetic field, *Journal of the Taiwan Institute of Chemical Engineers*, 45, 2014, 40-49.
- [23] Salem, A.M., Ismail, G., Fathy, R., Hydromagnetic flow of Cu water nanofluid over a moving wedge with viscous dissipation, *Chinese Physics B*, 23, 2014, 044402.
- [24] Sudarsana Reddy, P., Chamkha, A.J., Soret and Dufour Effects on MHD Convective Flow of Al₂O₃-Water and TiO₂-Water nanofluids past a stretching sheet in porous media with heat generation/absorption, *Advanced Powder Technology*, 27(4), 2016, 1207-1218.
- [25] Chamkha, A.J., Rashad, A. M., Natural convection from a vertical permeable cone in a nanofluid saturated porous media for uniform heat and nanoparticles volume fraction fluxes, *International Journal of Numerical Methods for Heat and Fluid Flow*, 22(8), 2012, 1073-1085.



- [26] Chamkha, A.J., Al-Mudhaf, A.F., Pop, I., Effect of heat generation or absorption on thermophoretic free convection boundary layer from a vertical flat plate embedded in a porous medium, *International Communications in Heat and Mass Transfer*, 33(9), 2006, 1096-1102.
- [27] Turkiymazoglu, M., Multiple solutions of heat and mass transfer of MHD slip flow for the viscoelastic fluid over a stretching sheet, *International Journal of Thermal Sciences*, 50, 2011, 2264-2276.
- [28] Hamad, M.A.A., Analytical solution of natural convection flow of a nanofluid over a linearly stretching sheet in the presence of the magnetic field, *International Communications in Heat and Mass Transfer*, 38, 2011, 487-492.
- [29] Sheikholeslami, M., Bandpy, M.G., Ellahi, R., Zeeshan, A., Simulation of MHD CuO-water nanofluid flow and convective heat transfer considering Lorentz forces, *Journal of Magnetism and Magnetic Materials*, 369, 2014, 69-80.
- [30] Ibrahim, W., Makinde, O.D., Double-diffusive in mixed convection and MHD stagnation point flow of nanofluid over a stretching sheet, *Journal of Nanofluids*, 4(1), 2015, 28-37.
- [31] Magyari, E., Chamkha, A.J., Exact analytical results for the thermosolutal MHD Marangoni boundary layers, *International Journal of Thermal Sciences*, 47(7), 2008, 848-857.
- [32] Nadeem, S., Hag, R.U., Effect of Thermal Radiation for magnetohydrodynamic Boundary Layer Flow of a Nanofluid Past a Stretching Sheet with Convective Boundary Conditions, *Journal of Computational and Theoretical Nanoscience*, 11, 2013, 32-40.
- [33] Nadeem, S., Hag, R.U., MHD boundary layer flow of a nanofluid past a porous shrinking with thermal radiation, *Journal of Aerospace Engineering*, 28(2), 2015, 04014061.
- [34] Turkiymazoglu, M., Pop, I., Heat and mass transfer of unsteady natural convection flow of some nanofluids past a vertical infinite flat plate with radiation effect, *International Journal of Heat and Mass Transfer*, 59, 2013, 167-171.
- [35] Chamkha, A.J., Khaled, A.-R.A., Similarity solutions for hydromagnetic mixed convection heat and mass transfer for Hiemenz flow through porous media, *International Journal of Numerical Methods for Heat and Fluid Flow*, 10(1), 2000, 94-115.
- [36] Ramzan, M., Bilal, M., Time-dependent MHD nano-second grade fluid flow induced by the permeable vertical sheet with mixed convection and thermal radiation, *PLoS One*, 10(5), 2015, e0124929.
- [37] Hayat, T., Muhammad, T., Alsaedi, A., Alhuthali, M.S., Magnetohydrodynamic three-dimensional flow of a viscoelastic nanofluid in the presence of nonlinear thermal radiation, *Journal of Magnetism and Magnetic Materials*, 385, 2015, 222-229.
- [38] Hag, R.U., Nadeem, S., Khan, Z.H., Akbar, N.S., Thermal radiation and slip effects on MHD stagnation point flow of nanofluid over a stretching sheet, *Physica E: Low-dimensional Systems and Nanostructures*, 65, 2015, 17-23.
- [39] Lakshmi, S., Reddy, S., Effect of Radiation on Mixed Convection Flow of a Non-Newtonian Nanofluid over a Non-Linearly Stretching Sheet with Heat Source/Sink, *International Journal of Modern Eng. Research*, 3, 2013, 2675-2696.
- [40] Hayat, T., Muhammad, T., Shehzad, S. A., Alsaedi, A., Similarity solution to three-dimensional boundary layer flow of second grade nanofluid past a stretching surface with thermal radiation and heat source/sink, *AIP Advances*, 5, 2015, 017107.
- [41] Malvandi, A., Hedayati, F., Nobari, M. R. H., An HAM analysis of the stagnation-point flow of a nanofluid over a porous stretching sheet with heat generation, *Journal of Applied Fluid Mechanics*, 7(1), 2014, 135-145.
- [42] Kahar, A., Kandasamy, R.R., Muhaimin, I., Scaling group transformation for the boundary-layer flow of a nanofluid past a porous vertical stretching surface in the presence of chemical reaction with heat radiation, *Computers & Fluids*, 52, 2011, 15-21.
- [43] Rashidi, M.M., Chamkha, A.J., Keimanesh, M., Application of multi-step differential transform method on the flow of a second-grade fluid over a stretching or shrinking sheet, *American Journal of Computational Mathematics*, 1(2), 2011, 119-128.
- [44] Sheikholeslami, M., Ganji, D. D., Heated permeable stretching surface in a porous medium using nanofluids, *Journal of Applied Fluid Mechanics*, 7(3), 2014, 535-542.
- [45] Takhar, H.S., Chamkha, A.J., Nath, G., MHD flow over a moving plate in a rotating fluid with the magnetic field, Hall currents and free stream velocity, *International Journal of Engineering Science*, 40(13), 2002, 1511-1527.
- [46] Chamkha, A.J., Coupled heat and mass transfer by natural convection about a truncated cone in the presence of magnetic field and radiation effects, *Numerical Heat Transfer, Part A: Applications*, 39(5), 200, 511-530.
- [47] Sharma, R.P., Seshadri, R., Mishra, S.R., Manjum, S.R., Effect of thermal radiation on the magnetohydrodynamic three-dimensional motion of a nanofluid past a shrinking surface under the influence of a heat source, *Heat Transfer*, 48(6), 2019, 2105-2121.
- [48] Hayat, T., Imtiaz, M., and Alsaedi, A., MHD 3D flow of a nanofluid in the presence of convective conditions, *Journal of Molecular Liquids*, 212, 2015, 203-208.
- [49] Zheng, L., Niu, J., Zhang, X., Gao, Y., MHD flow and heat transfer over a porous shrinking surface with velocity slip and temperature jump, *Mathematical and Computer Modelling*, 56, 2012, 133-144.
- [50] Gherasim, I., Roy, G., Nguyen, C.T., Vo-Ngoc D. Experimental investigation of nanofluids in confined laminar radial flows, *International Journal of Thermal Sciences*, 48, 2009, 1486-1493.
- [51] Angue Mintsu, H., Roy, G., Nguyen, C.T., Doucet, D., New temperature-dependent thermal conductivity data for water-based nanofluids, *International Journal of Thermal Sciences*, 48, 2009, 363-371.

ORCID iD

R.P. Sharma  <https://orcid.org/0000-0002-3359-1316>

S.R. Mishra  <https://orcid.org/0000-0002-3018-394X>



© 2022 Shahid Chamran University of Ahvaz, Ahvaz, Iran. This article is an open access article distributed under the terms and conditions of the Creative Commons Attribution-NonCommercial 4.0 International (CC BY-NC 4.0 license) (<http://creativecommons.org/licenses/by-nc/4.0/>).

How to cite this article: Sharma R.P., Mishra S.R. Metal and Metallic Oxide Nanofluid over a Shrinking Surface with Thermal Radiation and Heat Generation/Absorption, *J. Appl. Comput. Mech.*, 8(2), 2022, 557-565.
<https://doi.org/10.22055/JACM.2020.32813.2085>

Publisher's Note Shahid Chamran University of Ahvaz remains neutral with regard to jurisdictional claims in published maps and institutional affiliations.

